Cement & Concrete Composites 34 (2012) 911–916

Contents lists available at SciVerse ScienceDirect

Cement & Concrete Composites

journal homepage: www.elsevier.com/locate/cemconcomp

Quantitative correlations among textural characteristics of C–S–H gel and mechanical properties: Case of ternary Portland cements containing activated paper sludge and fly ash

S. Goñi [a,*], M. Frias [a], I. Vegas [b], R. García [c], R. Vigil de la Villa [c]

[a] Instituto de Ciencias de la Construcción Eduardo Torroja (IETcc-CSIC), C/Serrano Galvache, 4, 28033 Madrid, Spain
[b] Tecnalia, NANOC, Unidad Asociada CSIC-TECNALIA, Parque Tecnológico de Bizkaia, C/Geldo, 48160 Derio, Spain
[c] Dpto. de Geología y Geoquímica, Unidad Asociada CSIC-UAM, Universidad Autónoma de Madrid, 28049 Madrid, Spain

ARTICLE INFO

Article history:
Received 11 April 2011
Received in revised form 25 April 2012
Accepted 6 May 2012
Available online 11 May 2012

Keywords:
Calcium–silicate–hydrate (C–S–H)
Surface area
Compressive strength
Ternary blended cement
Activated paper sludge
Fly ash

ABSTRACT

The hydraulic activity of ternary Portland cements containing different proportions of commercial thermally activated paper sludge (APS(I)) and fly ash (FA) from coal combustion was evaluated from the textural characterization of the C–S–H gels formed during hydration. The study was accomplished by means of the specific surface area (SSA) and pore-size distribution (PSD), which were measured by the sorption isotherms of nitrogen gas and the BET method. The microstructure was characterized by scanning electron microscopy (SEM). The incorporation of such admixtures (APS and FA) clearly revealed an increase in both porosity and SSA. This effect decreased with the progress of hydration, together with a refinement of the nano-porous structure of C–S–H. In addition, high correlations were found between nano-structural characteristics of the C–S–H gel and mechanical compressive strengths.

1. Introduction

It is well known that the C–S–H gel is responsible for the cohesion of the cement paste and consequently determines mechanical properties to a great extent. This is due to the intrinsic characteristics of the gel texture in which the nanoparticles and assembly possibilities, among others, will play a key role in the engineering properties [1–9]. However, there are few precedents for which such basic principles are quantitatively correlated; i.e. between nanostructural characteristics and macro-engineering properties [10,11]. Thus, the core objective of this work was to establish such a correlation in the case of C–S–H gel formed during hydration of new types of ternary Portland cements containing thermally activated paper sludge (APS) and fly ash (FA) from coal combustion, which exhibit high pozzolanicity [12,13].

Two types of thermally activated paper sludge (APS) were used: (a) one manufactured at laboratory scale (APS(L)), which was activated at 700 °C for 2 h, in order to-eliminate the organic material, to achieve the total dehydroxylation of kaolinite into metakaolinite (MK), as well as to avoid an excessive decarbonation of calcite which could result in a significant amount of quicklime, compound well known by its expansive property [14] and (b) the other was obtained at industrial scale (APS(I)) based on the CDEM process [15]. In this process, paper sludge is subjected to controlled temperature (≈730 °C) in a fluidized bed in order to activate the latent pozzolanic properties in the raw waste. The combustion of organic waste generates sufficient energy to ensure that the automatic operation of the process without added contribution of fossil fuel. In addition, thermal energy is recovered in vapour exchanger. This steam drives the turbines for electricity generation. Suspended in the flue gases, fine particles can be found. Once captured in the corresponding filters, a mineral by-product, registered under the name "Topcrete" with pozzolanic properties, is provided. This product is a stable, non-toxic mineral that can be used as a high performance, zero carbon admixture to cement based materials. The material is mainly composed of meta-kaolin, calcium compounds and other minerals.

APS can be used as a supplementary cementing material leading to significant reductions in clinker without compromising functional performance levels. The production of Portland cement currently generates 0.8 tonnes of CO_2 emitted during the production of each tonne of Portland cement. Therefore, the partial replacement of Portland cement by novel mineral admixtures contributes to reducing CO_2 emissions associated with $CaCO_3$ decomposition during clinker burning.

* Corresponding author.
E-mail address: sgoni@ietcc.csic.es (S. Goñi).

0958-9465/$ - see front matter © 2012 Elsevier Ltd. All rights reserved.
http://dx.doi.org/10.1016/j.cemconcomp.2012.05.002

A preliminary work on the pozzolanic activity of ternary APS–FA–$Ca(OH)_2$ system showed higher pozzolanic activity of APS(L)–FA blends, mainly during the first 28 days of reaction, with respect to APS(I)–FA blends [16].

When such pozzolanic by-products were blended with ordinary Portland cement (OPC) instead of portlandite ($Ca(OH)_2$), the high pozzolanic activity of the APS(L)–FA–OPC system was also confirmed [17]. The mechanical compressive and flexural strengths were higher than the dilution effect for all the studied proportions and hydration times. This fact was also noticeable for the textural characteristics of the C–S–H gel formed during hydration reaction, evidencing important direct linear quantitative correlations among the textural parameters, nanoporosity and mechanical compressive strength.

On the basis of that previous work [17], this paper deals with the hydraulic activity of ternary Portland cements, containing different proportions of industrial thermally activated paper sludge (APS(I)) and fly ash (FA) from coal combustion. It is evaluated by combining the textural characterization of the C–S–H gels formed during hydration and mechanical behaviour.

The textural parameters were studied in the pastes by means of N_2 sorption isotherms, by applying the BET theory at 1, 7, 28 and 90 days. The texture results were quantitatively correlated with the compressive and flexural mechanical strength determined in the equivalent mortar specimens. The morphology of the C–S–H particles was studied by scanning electron microscopy (SEM).

2. Experimental

2.1. Sample preparation

Different ternary mixtures of APS(I)–FA–OPC were used, whose XRD patterns are shown in Fig. 1. Further details of the characterization of the raw materials can be found in Ref. [12]. APS(I) and FA pozzolans were previously mixed with a ratio of 1:1 by weight and subsequently partial replacements of OPC by 6%, 21%, 35% and 50% of pozzolan blends were made. The corresponding ternary APS(I)–FA–OPC mixtures were called as 0–100, 6–94, 21–79, 35–65 and 50–50 (see Table 1). Blended cement pastes were prepared at a demineralised water/binder ratio of 0.5. After mixing, a series of six prisms were moulded into 1 cm × 1 cm × 6 cm samples and compacted by vibration. The samples were demolded after 1 day at >95% rh and cured at 21 °C under >95% rh in sealed containers for a period ranging from 1 to 90 days. A portion of the samples were then cut into approximately 7 mm monolithic pieces. Nanoscale (1–100 nm) gel characterization was performed using the BET surface area and pore volume analysis. The monolithic pieces were first dried, according to the international standard ISO 9277 and 8213, at room temperature in desiccators with silica gel. They

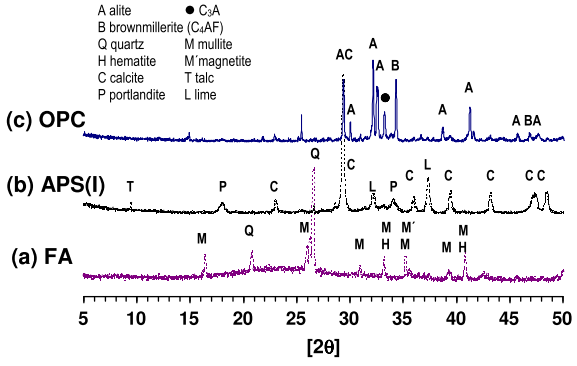

Fig. 1. XRD patterns of raw FA, APS(I) and OPC.

Table 1
Mixture proportions.

	APS(I) (% by weight)	FA (% by weight)	OPC (% by weight)
0–100	0	0	100
6–94	3	3	94
21–79	10.5	10.5	79
35–65	17.5	17.5	65
50–50	25	25	50

were dried until a constant weight was obtained, to eliminate free water (evaporable water), and then about 0.5 g of sample was degasified at 60 °C (to prevent decomposition of C–S–H gel) under vacuum (up to 5 μm Hg) and a cold trap of liquid nitrogen.

Concerning mechanical strength assessment, the mix proportions of mortars was based on the specifications and criteria established in UNE EN 196-1 regarding cement test methods. Thus, the water/binder ratio was of 1:2 and the binder/sand was of 1:3. After the initial curing period, specimens were demolded and stored in water (21 °C) at 1, 7, 28 and 90 days.

2.2. Apparatus

Surface-area measurements were made by the BET multipoint method (Model ASAP 2010, Micromeritics Instrument Corp., Norcross, GA), using N_2-77 K gas. The surface areas were calculated from the sorption isotherm data, using the BET method [18] in the relative pressure range of 0.003–0.3. Pore volume and pore-size distributions were calculated according to the Barret–Joyner–Halenda (BJH) method [19] using data from the adsorption isotherm branch. The Harkins and Jura [20] equation was used for calculating the thickness (t) of the adsorbed layer on the pore walls at every P/Po:

$$t = [13.99/0.034 - \log_{10}(P/Po)]^{1/2} \quad (1)$$

Mechanical strengths were determined by using Ibertest equipment.

The morphology of the hydrated compounds was determined with a scanning electron microscopy with the FEI INSPECT microscope equipped with an energy dispersive X-ray analyser (EDX). The powder samples were fixed to the metallic slide using a graphite plate in a BIO-RAD model SC 502. The EDX semiquantitative analysis was carried out with a silicon/lithium detector and a DX4i analyser. The analyser was first calibrated with a multimineral sample. The values of punctual analyses from different zones in the same sample were averaged.

3. Results and discussion

3.1. BET-N_2 Surface area and pore-size distribution

The isotherms of the pastes are like those of Fig. 2 which correspond to the 0–100 and 50–50 pastes (APS(I) + FA)/OPC) hydrated for 1 and 90 days. According to the IUPAC classification, the isotherms are type IV, which are typical for mesoporous materials, where the hysteresis loop is associated with the occurrence of pore condensation. The hysteresis loop is type H2, which is typical of disordered connected pore systems with distribution of pore-size and shape not well defined [21]. As it can be seen, the volume of N_2 adsorbed increases with hydration time (comparing 1 day and 90 days). This behaviour can be attributed to the amount and type of hydration products, mainly to the C–S–H gel formation.

The effect of the APS(I)–FA addition to the OPC is clearly manifested by an increase in both the volume of N_2 adsorbed and the

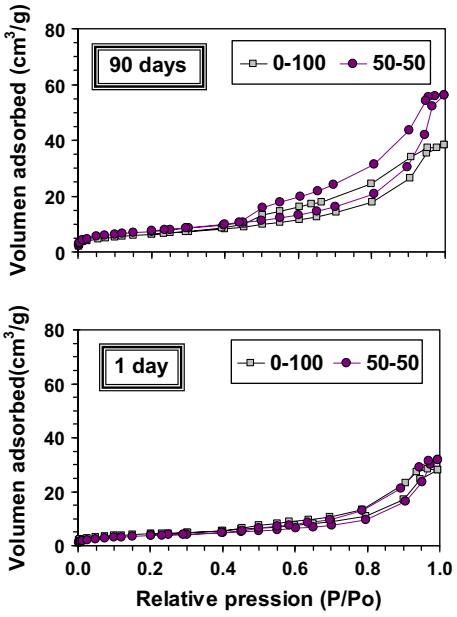

Fig. 2. Influence of the APS(I) + FA addition on the N_2 sorption isotherms after 1 and 90 days of hydration.

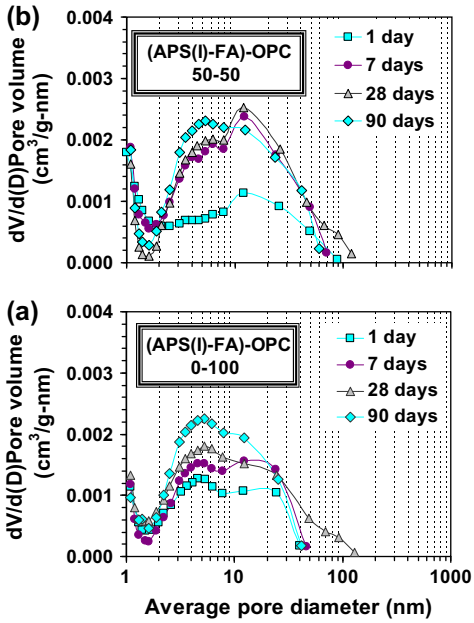

Fig. 4. Influence of the APS(I) + FA addition on the pore-size distribution curves of hydrated pastes.

hysteresis loop, revealing higher amount of both hydrated products and pores.

For the surface area (SA) (Fig. 3), the effect of the APS(I)–FA addition to the OPC depends on the hydration time. At early ages (1 day), low variations of SA are observed up to 35% of addition, decreasing thereafter for 50%. For longer ages (7–90 days), the SA values decreased from 0% to 6% of addition, increasing thereafter with the percentage of addition up to 35% where a plateau is reached.

The pore-size distribution (PSD), in the range of pores between 1 and 100 nm of diameter (Fig. 4) shows, in all the cases, a bi-modal distribution with two maxima centred at ~12 nm and ~5 nm.

In control cement paste (0–100) (Fig. 4a), the intensity of the signal centred at ~5 nm was slightly higher than that centred at ~12 nm throughout the hydration period. The effect of the addition (50–50) (Fig. 4b) was strongly marked by an increase in the intensity of both zones, which were also better defined at ~5 nm and ~12 nm. From 1 day to 28 days of hydration the proportion of ~12 nm pores is slightly higher than that of 5 nm. After 90 days, the proportion of pores of ~5 nm of diameter is higher than that of ~12 nm.

The existence of this bimodal population of size of pores of C–S–H gels matches well with the findings already reported by Thomas and Jennings [9] for ordinary Portland cements and those reported by Guerrero et al. [10] for belite cements. According to these works the two populations of pores might correspond to the LP C–S–H and the LD C–S–H states respectively.

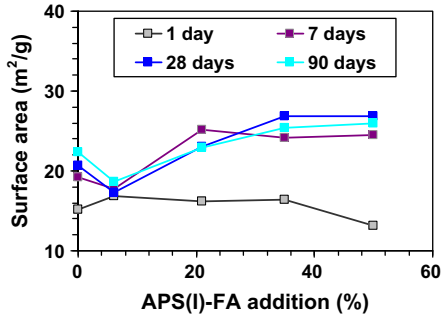

Fig. 3. Influence of the APS(I) + FA addition on the surface area.

3.2. SEM/EDX

The different morphologies of the hydrated compounds and the corresponding quantitative microanalyses at 90 days of curing can be seen in Fig. 5 and Tables 2 and 3. In the case of the 35–65 (APS(I)–FA)–OPC blend, typical cenospheres of FA together with alite particles (C_3S) with laminar morphogenesis and CSH gels can be identified (Fig. 5a). Also, prismatic ettringite formation inside the holds and laminar LDH compounds are observed in Fig. 5b [22,23].

When the pozzolan (APS + FA)/cement proportion was 50–50%, by SEM can clearly identify laminar aluminate hydrates (Fig. 5c), ettringite with prismatic morphology, forming spheres, and LDH compounds close to alite and portlandite pseudo hexagonal forms (Fig. 5d).

3.3. Quantitative correlation among textural parameters and mechanical strength

The changes of the compressive mechanical strength (CMS) as a function of the hydration time and percentage of addition are presented in Fig. 6. As expected, the CMS values decrease with the percentage of addition, except for the 6% of addition, whose values are fairly similar to those of plain OPC (0–100). To differentiate the effect of the pozzolanic activity of the additions on their mechanical behaviour, the relative values are represented in Fig. 7 as a function of the percentage of addition. The relative values were calculated by dividing the measured parameters by those corresponding to the 0–100 blend. The black line (inert dilution line) on the figure corresponds to the CMS values which, would have been obtained for inactive additions; in this case, the slope of the inert line has the value of 1. The 100 value of CMS corresponds to 0% of addition.

As it can be seen in Fig. 7, the experimental values are above the line of inert dilution up to the 35% of addition, revealing the pozzo-

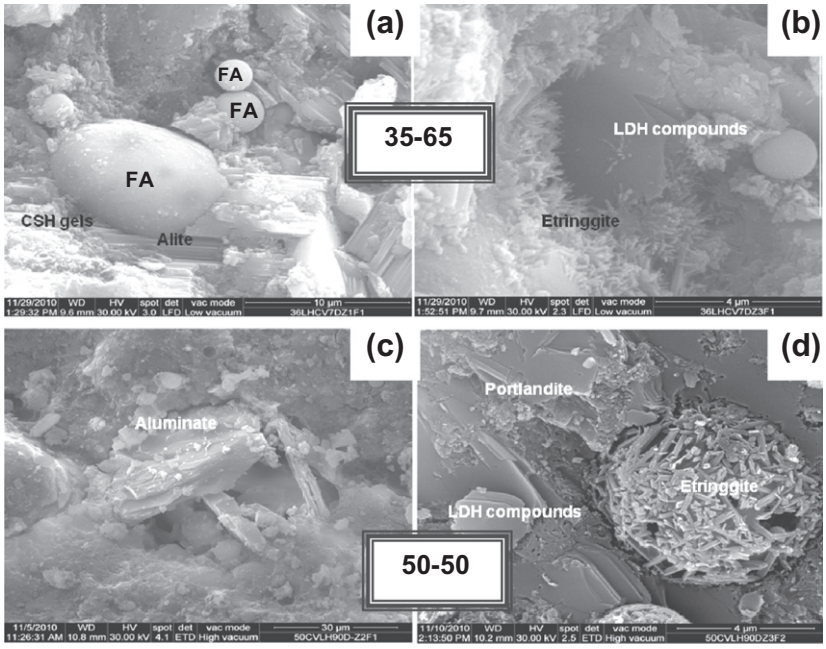

Fig. 5. SEM micrographs of principal hydrated compounds.

Table 2
Analysis by EDX (Fig. 5a and b).

Oxides (%)	CSH gels	Ettringite	Alite	LDH compounds
Al_2O_3	8.7 ± 0.4	39 ± 1	4.3 ± 0.4	13.9 ± 0.8
SiO_2	20.9 ± 0.8	24 ± 2	30 ± 1	26.9 ± 0.6
MgO	1.6 ± 0.4	–	1.6 ± 0.1	–
SO_3	–	2.2 ± 0.3	–	3.8 ± 0.3
CaO	59 ± 2	33 ± 2	61.2 ± 0.9	54 ± 1
Fe_2O_3	9.5 ± 0.2	1.6 ± 0.2	2.6 ± 0.6	2.1 ± 0.4

lanic activity of the APS(I)–FA blend. Replacements of 50% cement by APS(I)–FA admixtures bring out that relative CMS decreases.

For comparative purpose, the variation of the compressive and flexural strength values with hydration time as a function of the type of APS is presented in Fig. 8. The APS(L)–FA addition reaches higher compressive and flexural strength values than those of the APS(I)–FA throughout the hydration period, and especially at 90 days. The pozzolanic activity of the APS(L)–FA addition is clearly manifested in its mechanical behaviour because the compressive strength values are higher than those of the inert dilution effect.

The different pozzolanic activities of the two APS–FA additions was also corroborated by another technique such as the X-ray diffraction (XRD) (Fig. 9), where the portlandite ($Ca(OH)_2$) decreases more than the inner dilution effect for the 50% of APS(L) + FA addition, as a consequence of the pozzolanic reaction.

As it was above mentioned, the C–S–H gel is the responsible for the mechanical properties of hydrated cement-based materials;

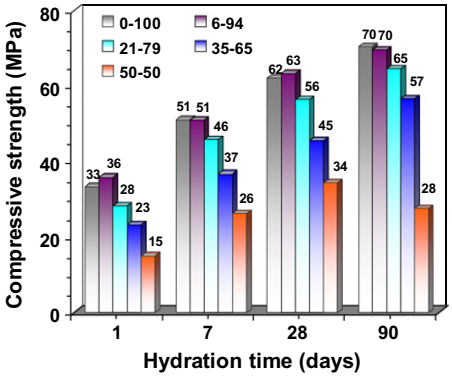

Fig. 6. Influence of the APS(I) + FA addition on the compressive strength.

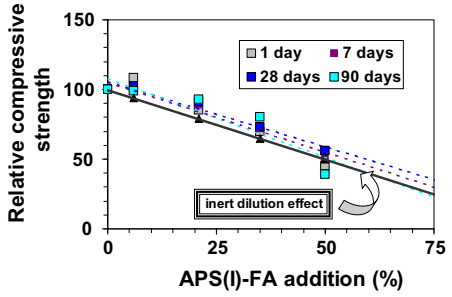

Fig. 7. Relative compressive strength of the APS(I) + FA addition: pozzolanic effect.

Table 3
Analysis by EDX (Fig. 5c and d).

Oxides (%)	Ettringite	C–S–H gels	Aluminate	LDH compounds	Portlandite
Al_2O_3	38 ± 1	6.3 ± 0.6	32 ± 1	16.8 ± 0.5	–
SiO_2	28 ± 1	25.5 ± 0.9	2.03 ± 0.09	30.2 ± 0.4	–
MgO	1.5 ± 0.3	1.1 ± 0.1	–	–	–
SO_3	3.1 ± 0.2	–	3.9 ± 0.4	3.4 ± 0.3	–
CaO	26 ± 2	65 ± 1	60 ± 2	47 ± 2	100
Fe_2O_3	2.4 ± 0.4	1.73 ± 0.08	0.9 ± 0.1	2.4 ± 0.2	–

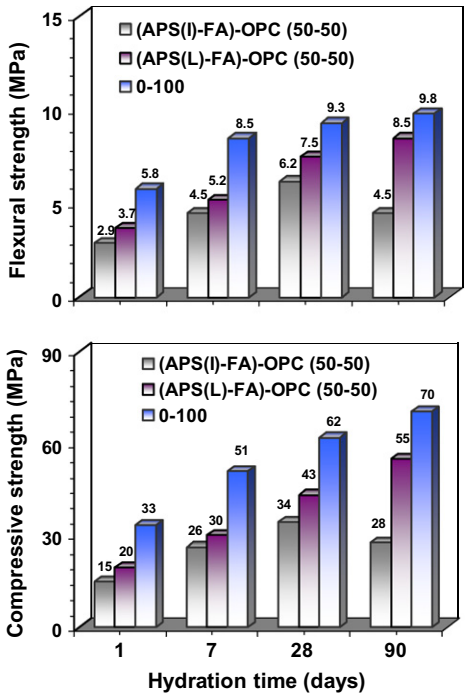

Fig. 8. Comparison of the 50–50 APS(I) + FA and APS(L) + FA additions on the compressive and flexural strengths at different hydration times.

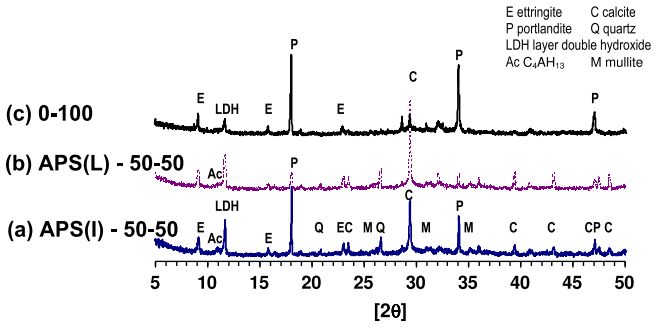

Fig. 9. Comparison of XRD patterns of hydrated cement pastes.

therefore, correlations can be expected between the macro-engineering properties and nano-texture characteristics of C–S–H gel.

This approach is presented in Fig. 10, where the experimental results of compressive mechanical strength (CMS), obtained from mortars (standardized prismatic specimens of $4 \times 4 \times 16$ cm) are related to those of SSA and percentage of nano-pores of ~5 nm and ~12 nm diameter, obtained from blended cement pastes.

As it can be seen, important direct linear quantitative correlations among the textural parameters such as SSA, LP, LD-C–S–H gels of pastes and mechanical compressive strength of mortars are found for both 0–100 and (APS(I)–FA)–OPC (50–50) blend. Unlike suggested previously, the LP C–S–H gel also exhibits a pivotal role in the compressive and flexural strength.

In the case of 50–50 blend, the slopes of the regressions are lower (about 50% lower than those of the 0–100 case). For the values corresponding to the APS(L) addition (included for comparison), there is a change of tendency, where at early ages the SSA and porosity increase with the CMS and then decrease. At longer ages the values tend to be located on the regression line of the plain OPC (0–100). The change of tendency can be attributed to the higher pozzolanic activity of the APS(L) addition, which induces larger amount of pozzolanic products leading to a decrease in the porosity of gels.

4. Conclusions

1. According to the data obtained from adsorption isotherms of N_2-77, the C–S–H gels of ternary APS(I)–FA–OPC exhibit a bimodal pore-size distribution with defined pore sizes of ~12 nm and ~5 nm.
2. The existence of 12-nm and 5-nm sized pores is attributed to different packing of the basic units of C–S–H gel; namely the loose packing (LP) (12 nm) gel and the low density (LD) (5 nm) gel.
3. The SEM/EDX analysis identified clearly the typical morphologies of the main hydrated phases: CSH gels, ettringite and LDH compounds.
4. The relative compressive strength values of the blended cement mortars decreased with the increasing pozzolan mix content. The replacement of 50% of pozzolan blend presented an important dilution effect, similar to an inert behaviour.
5. The proportion of both types of C–S–H gel (LP and LD) depends on the percentage of APS(I) + FA addition. In the absence of APS(I) + FA addition, the proportion of pores of ~5 nm is higher than that of ~12 nm. The addition caused that C–S–H gel develops both types in higher proportion than those of plain OPC (0–100), with a higher contribution of pores of ~12 nm to respect those of ~5 nm. This tendency changed after 90 days, where the contribution of pores of ~5 nm is higher than that of ~12 nm.
6. Important direct linear quantitative correlations among the textural parameters such as SSA, LP, LD-C–S–H gels of pastes and mechanical compressive strength of mortars are found.
7. Unlike suggested previously, the LP C–S–H gel also exhibits a pivotal role in the compressive and flexural strength.

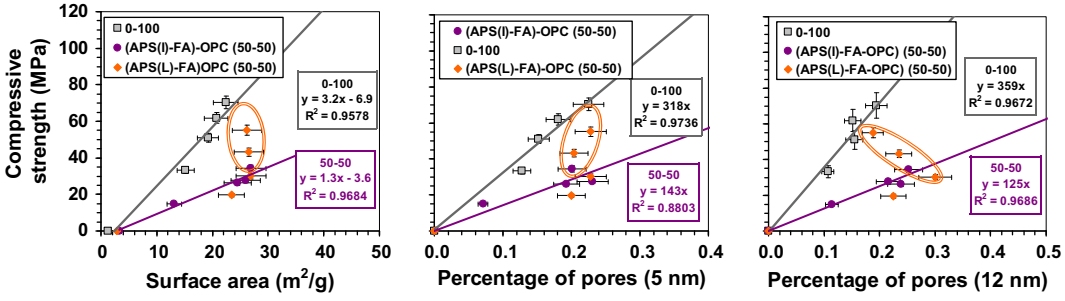

Fig. 10. Quantitative correlations among the surface area, nanoporosity and mechanical compressive strength of APS(I).

Acknowledgements

The authors gratefully acknowledge the financial support by the Minister of Science and Technology MAT2009-10874-CO3 and to the Homen Paper Madrid company, CDEM and Spanish Cement Institute (IECA) for their help in this project.

References

[1] Jönsson Bo, Nonat A, Labbez C, Cabane B, Wennerström H. Controlling the cohesion of cement paste. Langmuir 2005;21:9211–21.
[2] Plassard C, Lesniewska E, Pochard I, Nonat A. Nanoscale experimental investigation of particle interactions at the origin of the cohesion of cement. Langmuir 2005;21:7263–70.
[3] Rarick RL, Bhatty JI, Jennings HM. Surface area measurements using gas sorption: application to cement paste. In: Skalny J, Mindess S, editors. Materials science of concrete IV. The American Ceramic Society; 1995. p. 1–39.
[4] Powers TC, Brownyard TL. Studies of the physical properties of hardened Portland cement paste. Skokie (IL, USA): Portland Cement Association R&D Bull. Reprinted from J Amer Concr Inst 1946;18(2):101–132 and 1948; 8(5):549–602
[5] Powers TC. The physical structure and engineering properties of concrete. Chicago: Portland Cement Association R&D Bull.; 1958.
[6] Brunauer S. Tobermorite gel – the heart of concrete. Am Sci 1962;50(1):211–29.
[7] Feldman RF, Sereda PJ. A model for hydrated Portland cement paste as deduced from sorption length change and mechanical properties. Mater Struct 1968;1(6):509–20.
[8] Feldman RF, Sereda PJ. A new model for hydrated Portland cement and its practical implications. Eng J Can 1970;53(8/9):53–9.
[9] Thomas JJ, Jennings HM. A colloidal interpretation of chemical aging of the C–S–H gel and its effects on the properties of cement paste. Cem Concr Res 2006;36:30–8.
[10] Guerrero A, Goñi S, Dolado JS. Belite cements. Modifications of the C–S–H gel by alkaline hydrothermal activation.. ACI Mater J 2009(April):138–43.
[11] Frías M, Rodríguez L, García R, Vegas I. Influence of activation temperature on reaction kinetics in recycled clay waste-calcium hydroxide systems. J Am Ceram Soc 2008;91(12):40-41–4051.
[12] Frías M, Sánchez de Rojas MI. Microstructural alterations in fly ash mortars: study on phenomena affecting particle and pore size. Cem Concr Res 1997;27(4):619–28.
[13] Goñi S, Guerrero A, Puertas F, Hernández MS, Palacios M, Dolado JS, et al. Textural and mechanical characterization of C–S–H gels from hydration of synthetic T1-C3S, β-C2S and their blends. Mater Construcc 2011;61(302):169–83.
[14] Frías M, Sánchez de Rojas MI, Rodriguéz O, García R, Vigil R. Characterisation of calcined paper sludge as an environmentally friendly source of MK for manufacture of cementitious materials. Adv Cem Res 2008;20(1):23–30.
[15] International Patent. A Method of preparing a pozzolanic material form paper residue and a method for the manufacture of cement from said material. No. WO 279 96/06057; 1996.
[16] Frías M, García R, Vigil de la Villa R, Villar E. The effect of binary pozzolan mix on the mineralogical changes in the ternary activated paper sludge–fly ash–$Ca(OH)_2$ system. Constr Build Mater, CONBUILDMAT-D-12-137; submitted for publication.
[17] Goñi S, Frias M, Vegas I, García R, Vigil R. Effect of ternary cements containing thermally activated paper sludge and fly ash on the texture of C–S–H gel. Constr Build Mater 2012;30:381–8.
[18] Brunauer S, Emmett PH, Teller E. Adsorption of gases in multimolecular layers. J Am Chem Soc 1938;60:309–19.
[19] Barret EP, Joyner LG, Halenda PP. The determination of pore volume and area distributions in porous substances. J Am Chem Soc 1951;73:373–81.
[20] Harkins WD, Jura G. Vapor adsorption method for the determination of the area of a solid without the assumption of a molecular area, and the areas occupied by nitrogen and other molecules on the surface of a solid. J Am Chem Soc 1944;66:1366–73.
[21] Lowell S, Shields JE, Thomas MA, Thommes M. Characterization of porous solids and powers: surface area, pore size and density. Kluwer Academic Publishers; 2004.
[22] Vigil R, Rodríguez O, García R, Frías M. Mineral phases in an activated kaolinitic waste blended cement system. Appl Clay Sci 2010;50(1):137–42.
[23] Fernández R, Nebreda B, Vigil R, García R, Frías M. Mineralogical and chemical evolution of hydrated phases in the pozzolanic reaction of calcined paper sludge. Cem Concr Compos 2010;32(10):775–82.